Advances in Nano Research, *Vol. 8 No. 2 (2020) 169-182*
DOI: https://doi.org/10.12989/anr.2020.8.2.169

Dynamic characteristics of hygro-magneto-thermo-electrical nanobeam with non-ideal boundary conditions

Farzad Ebrahimi*[1], Mohammadreza Kokaba[1], Gholamreza Shaghaghi[2] and Rajendran Selvamani[3]

[1] *Mechanical Engineering Department, Engineering Faculty, Imam Khomeini International University, Qazvin, Iran*
[2] *Young Researchers and Elites Club, Science and Research Branch, Islamic Azad University, Tehran, Iran*
[3] *Department of Mathematics, Karunya University, Coimbatore 641114, Tamil nadu, India*

(*Received April 5, 2019, Revised January 11, 2020, Accepted January 19, 2020*)

Abstract. This study presents the hygro–thermo–electromagnetic mechanical vibration attributes of elastically restrained piezoelectric nanobeam considering effects of beam surface for various elastic non-ideal boundary conditions. The nonlocal Eringen theory besides the surface effects containing surface stress, surface elasticity and surface density are employed to incorporate size-dependent effects in the whole of the model and the corresponding governing equations are derived using Hamilton principle. The natural frequencies are derived with the help of differential transformation method (DTM) as a semi-analytical-numerical method. Some validations are presented between differential transform method results and peer-reviewed literature to show the accuracy and the convergence of this method. Finally, the effects of spring constants, changing nonlocal parameter, imposed electric potential, temperature rise, magnetic potential and moisture concentration are explored. These results can be beneficial to design nanostructures in diverse environments.

Keywords: mechanical vibration; piezoelectric nanobeam; non-ideal boundary condition; size dependent effects

1. Introduction

Beams are very frequently used and common components in the mechanical and biomechanical design (Rao 2007). There are various beam theories in elasticity such as Euler-Bernoulli (EB), Timoshenko, Reddy, and Levinson (Aydogdu 2019). Euler-Bernoulli which is the oldest theory was firstly presented at the 18th century and the main assumption of this theory is that no deformations occur in the plane of the cross-section. Consequently, the in-plane rigid body displacement is considered to determine the governing equation. Since the carbon nanotube was discovered, many researches in the nano-scale structures area were started. Well-stablished researches showed that EB theory is naturally inadequate to apply for this type of structures (Wang *et al*. 2006, Marzbanrad *et al*. 2016, 2017).

Eringen developed a nonlocal continuum mechanics theory which assumes that the stress at a specified point is a function of strains at all other points in the media (Eringen 1983) In recent decades, many other nonlocal theories like couple stress theory and the strain gradient theory are evolved to explain the nonlocal continuum mechanics and size effect in the small-scale structures but particularly, the studies using Eringen's nonlocal elasticity theory have been the most attractive research field to investigate and analyze the bending, buckling, and vibration of nano structures (Park and Gao 2016). Ke *et al*. (2019) investigated the Nonlinear free vibration of embedded double-walled carbon nanotubes (DWNTs) based on Eringen's nonlocal elasticity theory and von Karman nonlinearity and illustrated the influences of nonlocal and geometrical parameters on the nonlinear free vibration of DWNTs. Reddy (2007) developed nonlocal theories for Euler-Bernoulli, Timoshenko, Reddy, and Levinson beams. Barari *et al*. (2018) investigated the non-linear vibration of Euler-Bernoulli beams subjected to the axial loads by means of iteration (VIM) and parametrized perturbation (PPM) methods.

Eltaher *et al*. (2013) used a finite element model to analyze EB beams and illustrated the effects of nonlocal parameters, higher modes and moments of inertia on the natural frequencies. Ebrahimi *et al*. (2014) presented a semi-analytical differential transformation method (DTM) for vibration analysis of size-dependent nanobeams based on nonlocal Timoshenko beam theory and showed the effect of small- scale parameters, mode number, aspect ratios and other geometrical specifications on the natural frequencies. It is noteworthy to mention that after exploring the piezoelectric nanostructure properties, many researchers have focused on the piezoelectric material. This kind of materials can convert nanoscale mechanical energy into the electrical energy. The effect of the piezoelectric coefficient on the ZnO nanowires was illustrated by Zhao *et al*. (2014). Li *et al*. (2014) studied the free vibration of a functionally graded piezoelectric beam using differential quadrature method and showed the impact of some material parameters on the natural frequency. Meanwhile a pin-moment model of flexoelectric actuators was presented by Wang *et al*. (2018) and an electro-hydrostatic actuator for hybrid active-

*Corresponding author, Professor,
E-mail: febrahimy@eng.ikiu.ac.ir

http://www.techno-press.org/?journal=journal=anr&subpage=5
ISSN: 2287-237X (Print), 2287-2388 (Online)

passive vibration isolation by Henderson *et al*. (2018). Also, Active vibration compensator on moving vessel by hydraulic parallel mechanism examined by Tanaka (2018).

Furthermore, in recent years many researchers have presented the static and dynamic characteristics of beams and plates exposed to hygro-thermal environments because of the considerable effects of these environments on the structure's behavior. Gayen and Roy (2013) presented an analytical method to determine the stress distributions in circular tapered laminated composite beams under hygro and thermal loadings. Ebrahimi and Barati (2017) studied hygro-thermo-mechanical vibration analysis of functionally graded size dependent nanobeams via differential transform method (DTM) and explored the effects of moisture concentration, temperature change, nonlocal parameter, etc., on the vibration of functionally graded beams with arbitrary boundary conditions.

In most above-mentioned researches, the ideal boundary condition assumption is considered in problem solving and any deviation is neglected. However, there are some small deviations from the ideal condition in real systems. Lee and Kim (2000) investigated Free vibration analysis of beams with non-ideal clamped boundary conditions. Pakdemirli and Boyaci (2003) analyzed the nonlinear vibration of the simply supported beam with non-ideal support and presented the variation of natural frequencies depending on the mode numbers and locations.

In this paper, Eringen nonlocal beam theory is used to investigate the hygro–thermo–electromagnetic mechanical vibration characteristic of nanobeam for non-ideal boundary conditions by considering surface effects. The governing equations and boundary conditions are obtained using Hamilton's principle and differential transformation method (DTM) is utilized to solve the governing equations. The convergence of numerical results is first investigated and validated with the peer-reviewed literature which are in good agreement. Finally, through some numerical examples, the effects of various parameters like the spring constant, nonlocal parameter, voltage, temperature change, magnetic potential and moisture concentration effects and non-ideal boundary condition are presented.

2. Governing equations

2.1 Eringen's Nonlocal elasticity theory

According to the nonlocal elasticity theory which provides information about the forces in micro and nano scales and between the atoms, the stress field at a point in an elastic medium depends not only on the strain field at that point but also on strains at all points of the configuration. This assumption was approved by many of experimental observations in small scales. Therefore, the nonlocal stress tensor and electric displacement by omitting the body forces for a homogeneous and piezoelectric solid at any point x in the bulk of material can be demonstrated as (Tounsi *et al*. 2013)

$$\sigma_{ij} - \mu^2 \nabla^2 \sigma_{ij} = C_{ijkl}\varepsilon_{kl} - e_{kij}E_k - \lambda_{ij}\Delta T \tag{1}$$

$$D_i - \mu^2 \nabla^2 D_i = e_{ikl}\varepsilon_{kl} + \varepsilon_{ik}E_k + p_i \Delta T \tag{2}$$

where σ_{ij}, D_i are the stress tensor and electric field components. ε_{kl}, C_{ijkl}, λ_{ij}, e_{ikl} are the strain, elastic constant, thermal module and surface piezoelectricity constants, respectively. ΔT and p_i are the temperature change and pyroelectric constant $\mu = (e_0 a)^2$ is the nonlocal constant, furthermore, e_0 is a material constant and a is the internal characteristic length.

2.2 Surface effect

Recent researches have demonstrated that some properties of nanostructures such as piezoelectric constant are very size dependent and this kind of dependency is attributed to the surface effects. Indeed, the energy of the atoms which belong to the layers of the surface, has some effect on the nanostructures mechanical properties (He and Lilley 2008, Schmid *et al*. 1995).

surface elasticity theory which proposed by Gurtin and Murdoch (1975) have been seriously adopted to model the surface effects on the properties of nanostructures and many other researchers have investigated the influence of surface effect on the vibration and buckling of nanostructures. Considering a two-dimensional surface layer with imperceptible thickness t is the main assumption in this theory. It should be noted that surface layer does not actually exist and is only because of modeling purposes.

It is experimentally proved that, the surface energy density depends on the in-plane strain at the surface. Furthermore, it is common to believe that in the piezoelectric nanostructures the surface energy density may also relies on the electric field at the surface (Friesen *et al*. 2001). If we write the Tylor expansion of surface energy density (Huang and Yu 2006), the following constitutive equations can be obtained

$$\tau^{sl}_{\alpha\beta} = \tau^0_{\alpha\beta} + C^s_{\alpha\beta\gamma\delta}\varepsilon_{\gamma\delta} + e^s_{\alpha\beta k}E_k \tag{3}$$

$$D^{sl}_i = D^0_i + e^s_{\alpha\beta i}E_i + \kappa^s_{ij}E_j \tag{4}$$

where $\varepsilon_{\gamma\delta}$ is surface strains. $C^s_{\alpha\beta\gamma\delta}$, $e^s_{\alpha\beta k}$ and k^s_{ij} are surface elastic, surface piezoelectric and surface dielectric constants respectively. $\tau^{sl}_{\alpha\beta}, \tau^0_{\alpha\beta}$ are the nonlocal stress tensor and residual surface stress tensor respectively.

By considering two above-mentioned surface layers with same material properties, the relative stress-strain relationship for surface layers will be explained as follows

$$\tau_{xx} = \tau_0 + E^s u_{x,x}, \quad E^s = 2\mu_0 + \lambda_0, \quad \tau_{nx} = \tau_0 u_{n,x} \tag{5}$$

The σ_{zz} which is often omitted in conventional beam theories will be taken into account to satisfy the equilibrium equations. This stress component has linear correlation within the beam thickness which expressed as

$$\boldsymbol{\sigma_{zz}} = \frac{\boldsymbol{2z\nu}}{\boldsymbol{h}}\left(\boldsymbol{\tau_o}\frac{\boldsymbol{\partial^2 w}}{\boldsymbol{\partial x^2}} - \boldsymbol{\rho_o}\frac{\boldsymbol{\partial^2 w}}{\boldsymbol{\partial t^2}}\right) \tag{6}$$

3. Problem formulation and solution

Based on the theoretical description and formulation which proposed in the previous section for nanostructures, the hygro-thermo-electromagnetic vibration of a size-dependent piezoelectric nanobeam with non-ideal boundary conditions is studied. A piezoelectric nanobeam with length L ($0 \le x \le L$), width b ($-b/2 \le y \le b/2$) and thickness h ($-h/2 \le z \le h/2$), induced to an applied voltage, magnetic field, moisture concentration, nonlocal parameters, surface effect and uniform temperature change ΔT. The Euler-Bernoulli beam theory with its specific assumptions is used to expand the case study. Based on the Euler-Bernoulli beam approach the nanobeam cross section is assumed to persist its plane configuration and normal to the deformed beam axis. The beam and the coordinate system are illustrated in Fig. 1.

Based on the Euler–Bernoulli beam theory, the displacement can be expressed as follows

$$u_1 = u - z\frac{\partial w}{\partial x}, \qquad u_2 = 0, \qquad u_3 = w(x,t) \tag{7}$$

where $u(x,t)$ and $w(x,t)$ are axial and lateral displacement components in middle plane of the beam and t is the time.

The non-zero longitudinal strain according to Euler-Bernoulli beam model can be stated as

$$\varepsilon_{xx} = \frac{\partial u}{\partial x} - z\frac{\partial^2 w}{\partial^2 x} \tag{8}$$

correspondingly, the surface stress (σ_s) and normal stress (σ_{xx}) which are the functions of surface strain ε_{xx}can be given as follows

$$\begin{aligned} \sigma_{xx} &= E\varepsilon_{xz} + \upsilon\sigma_{zz} - e_{31}E_z \\ \sigma_s &= \tau_0 + E_s\varepsilon_{xx} \end{aligned} \tag{9}$$

while e_{31} and E_z are the piezoelectric coefficient and z-component of the electric field, respectively. Furthermore, τ_0 and E_s are the surface tension and its Young's modulus.

The dispensation of electric field to satisfy Maxwell's equation can be defined as (Samaei *et al*. 2012)

$$\begin{aligned} &E_x = -\frac{\partial \phi}{\partial x}; \qquad E_z = -\frac{\partial \phi}{\partial x}; \\ &D_x = \lambda_{11}E_x; \qquad D_z = e_{31}\varepsilon_x + \lambda_{33}E_z; \\ &\frac{\partial D_x}{\partial x} + \frac{\partial D_z}{\partial z} = 0 \end{aligned} \tag{10}$$

where λ_{11} and λ_{33} exhibit the dielectric coefficients, D_x and D_z are electric displacements. Because of the λ_{11} and λ_{33} are in the identical order and concluding $E_x \ll E_z$, so D_x would be neglected in compare with D_z. by considering electrical boundary conditions as $\phi(x,-h) = 0$, $\phi(x,h) = 2V$ and substituting Eq. (8) into Eq. (10), the electrical potential is obtained as

$$\phi(x,z) = -\frac{e_{31}}{\lambda_{33}}\left(\frac{z^2 - h^2}{2}\right)\frac{\partial^2 w}{\partial x^2} + \left(1 + \frac{z}{h}\right)V \tag{11}$$

Finally, the effective axial load of the piezoelectric nanobeam can be shown as

$$P_{electric}(x,t) = b\int_{-h}^{h}\sigma_x^* dz = 2Vbe_{31} \tag{12}$$

piezoelectric property leads to σ_x^* which indicates the normal stress.

In order to obtain the governing equations, the Hamilton's principle is presented in the following

Form

$$\int_0^t \delta(U - T + W_{ext})dt = 0 \tag{13}$$

whereas, U, T and W_{ext} represent the strain energy, kinetic energy and work done by external forces.

The variation of strain energy is acquired as

$$\delta U = \int_0^L\int_{-\frac{h}{2}}^{\frac{h}{2}}\left(\begin{aligned} &\sigma_{xx}\delta\varepsilon_{xx} + \sigma_{xz}\delta\gamma_{xz} - D_x\delta E_x \\ &-D_z\delta E_z + K_{TL}w(0,t)\delta w(0,t) \\ &+K_{RL}\frac{\partial w(0,t)}{\partial x}\delta\left(\frac{\partial w(0,t)}{\partial x}\right) \\ &+K_{TR}w(L,t)\delta w(L,t) \\ &+K_{RR}\frac{\partial w(L,t)}{\partial x}\delta\left(\frac{\partial w(L,t)}{\partial x}\right) \end{aligned}\right)dzdx \tag{14}$$

Merging Eqs. (8) and (14) leads to

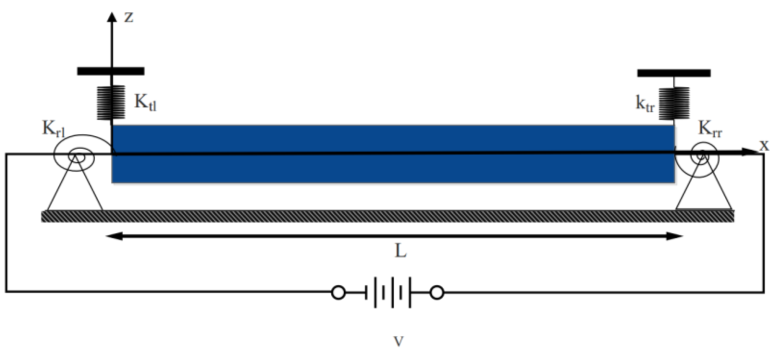

Fig. 1 Geometry of a nanobeam with length L and thickness h in elastic medium

$$\delta U=\int_0^l\int_{-h/2}^{h/2}\begin{bmatrix}N\delta u-M\delta\left(\frac{\partial^2 w}{\partial x^2}\right)+D_x\delta\left(\frac{\partial\phi}{\partial x}\right)\\+D_z\delta\left(\frac{\partial\phi}{\partial z}\right)+K_{TL}w(0,t)\delta w(0,t)\\+K_{RL}\frac{\partial w(0,t)}{\partial x}\delta\left(\frac{\partial w(0,t)}{\partial x}\right)\\+K_{TR}w(L,t)\delta w(L,t)\\+K_{RR}\frac{\partial w(L,t)}{\partial x}\delta\left(\frac{\partial w(L,t)}{\partial x}\right)\end{bmatrix}dx \tag{15}$$

where the axial force N and the bending moment M can be written as follows

$$N_x=\int_{-\frac{h}{2}}^{\frac{h}{2}}\sigma_{xx}\,dz\,,\qquad M_x=\int_{-\frac{h}{2}}^{\frac{h}{2}}\sigma_{xx}z\,dz \tag{16}$$

The kinetic energy for nanobeam can be determined as

$$\begin{aligned}T&=\frac{1}{2}\rho\iint(\dot{u}_1^2+\dot{u}_2^2+\dot{u}_3^2)\,dA.dx\\&=\frac{1}{2}\rho\int\left(I_1\left(\frac{\partial u}{\partial t}\right)^2+I_2\left(\frac{\partial^2 w}{\partial x\partial t}\right)^2+I_1\left(\frac{\partial w}{\partial t}\right)^2\right)dx\end{aligned} \tag{17}$$

where I_1 and I_2 are defined

$$I_1=\int_{-\frac{h}{2}}^{\frac{h}{2}}\rho dz,\qquad I_2=\int_{-\frac{h}{2}}^{\frac{h}{2}}\rho z^2dz \tag{18}$$

Accordingly, the first variation of Eq. (17) can be obtained as

$$\begin{aligned}\delta T=-\int_0^l\Bigg(&I_1\left(\frac{\partial^2 w}{\partial t^2}\right)\delta(w)-I_2\left(\frac{\partial^4 w}{\partial x^2\partial t^2}\right)\delta(w)\\&+I_1\left(\frac{\partial^2 u}{\partial t^2}\right)\delta(u)\Bigg)dx\end{aligned} \tag{19}$$

The magnetic force in conformance with magnetic field and magnetic potential can be expressed as

$$f_z=\eta H_x^2\left(\frac{\partial^2 w}{\partial x^2}\right) \tag{20a}$$

$$q_z=\int_A f_z dz=\eta A H_x^2\left(\frac{\partial^2 w}{\partial x^2}\right) \tag{20b}$$

$$N^H=-\int_A E\beta\Delta H dA=-E\beta\Delta H dA \tag{20c}$$

Finally, the work done by external forces is obtained as

$$\delta W_{ext}=\int_0^t(q_w\delta(w)+q_u\delta(u)) \tag{21}$$

where q_w is determined as

$$\begin{aligned}q_w=\big(&H+N_p+N_T+P_{electric}+K_P\\&+q_z+N^H\big)\left(\frac{\partial^2 W}{\partial x^2}\right)-K_wW\end{aligned} \tag{22}$$

In the above equation, N_p and N_T are the normal forces caused due to the biaxial force P_0 and temperature rise, and H is a constant obtained by residual surface stress and the configuration of beam cross-section.

$$\begin{aligned}N_P&=P_0\\N_T&=-\lambda_1A\Delta T\\H&=2b\tau_0\end{aligned} \tag{23}$$

Substituting Eqs. (15), (19), (21) into eq.(13) with setting the coefficient of δu and δw equal to zero, the following terms will be acquired

$$\frac{\partial N}{\partial x}+q_u-I_1\left(\frac{\partial^2 u}{\partial t^2}\right)=0 \tag{24}$$

$$\frac{\partial^2 M}{\partial x^2}+q_w+I_2\left(\frac{\partial^4 w}{\partial x^2\partial t^2}\right)-I_1\left(\frac{\partial^2 w}{\partial t^2}\right)=0 \tag{25}$$

The bending moment for piezoelectric nanobeam with taking into account the surface effects will be determined by

$$M=\int\sigma_{xx}zdA+\int\tau_{xx}zdA-\int e_{31}\phi_z zdA \tag{26}$$

$$\begin{aligned}M=&-(EI)^*\frac{\partial^2 w}{\partial x^2}+\frac{2I\nu}{h}\left(\tau_0\frac{\partial^2 w}{\partial x^2}-\rho_0\frac{\partial^2 w}{\partial t^2}\right)\\&+\frac{e_{31}^2}{\lambda_{33}}I\frac{\partial^2 w}{\partial x^2}\end{aligned} \tag{27}$$

where $(EI)^*=E\left(\frac{bh^3}{12}\right)+E_s\left(\frac{h^3}{6}+\frac{bh^2}{2}\right)$ is the effectual bending stiffness. Using the nonlocal elasticity theory for bending moment leads to

$$\begin{aligned}&M-\mu\frac{\partial^2 M}{\partial x^2}\\&=-(EI)^*\frac{\partial^2 w}{\partial x^2}+\frac{2I\nu}{h}\left(\tau_0\frac{\partial^2 w}{\partial x^2}-\rho_0\frac{\partial^2 w}{\partial t^2}\right)+\frac{e_{31}^2}{\lambda_{33}}I\frac{\partial^2 w}{\partial x^2}\end{aligned} \tag{28}$$

$$\begin{aligned}M=&\,\mu\left(-I_2\left(\frac{\partial^4 w}{\partial x^2\partial t^2}\right)+I_1\left(\frac{\partial^2 w}{\partial t^2}\right)-q_w\right)-(EI)^*\frac{\partial^2 w}{\partial x^2}\\&+\frac{2I\nu}{h}\left(\tau_0\frac{\partial^2 w}{\partial x^2}-\rho_0\frac{\partial^2 w}{\partial t^2}\right)+\frac{e_{31}^2}{\lambda_{33}}I\frac{\partial^2 w}{\partial x^2}\end{aligned} \tag{29}$$

Substituting Eq. (29) into Eq. (25) the constitutive equation of the motion will be procured

$$\begin{aligned}&\left(1-\mu\frac{\partial^2}{\partial x^2}\right)\left(-I_2\left(\frac{\partial^4 w}{\partial x^2\partial t^2}\right)+I_1\left(\frac{\partial^2 w}{\partial t^2}\right)-q_w\right)\\&-(EI)^*\frac{\partial^4 w}{\partial x^4}+\frac{2I\nu}{h}\left(\tau_0\frac{\partial^4 w}{\partial x^4}-\rho_0\frac{\partial^4 w}{\partial x^2\partial t^2}\right)\\&+\frac{e_{31}^2}{\lambda_{33}}I\frac{\partial^4 w}{\partial x^4}=0\end{aligned} \tag{30}$$

considering the harmonic movement for the free vibration of nanobeam with natural frequency of ω, that is

$$w(x,t) = W(x)e^{i\omega t} \tag{31}$$

Substituting Eq. (31) into Eq. (26) leads to final PDE equation of motion as follows

$$\begin{aligned}&\left(1-\mu\frac{\partial^2}{\partial x^2}\right)\left(\omega^2 I_2\left(\frac{\partial^2 W}{\partial x^2}\right)-\omega^2 I_1 W(x)-q_w\right)\\&-(EI)^*\frac{\partial^4 W}{\partial x^4}+\frac{2I\nu}{h}\left(\tau_0\frac{\partial^4 W}{\partial x^4}+\rho_0\omega^2\frac{\partial^4 W}{\partial x^2}\right)\\&+\frac{e_{31}^2}{\lambda_{33}}I\frac{\partial^4 W}{\partial x^4}=0\end{aligned} \tag{32}$$

4. Differential transformation method

DTM is a solution procedure for solving ordinary differential equations which determined from Taylor's series expansion. It uses a polynomial form that is sufficiently differentiable as an approximation to the exact solution. implementing DTM for solving free vibration problems, involves two transformations, namely, differential transformation (DT) and inverse differential transformation (IDT) which defined as follows

$$\boldsymbol{Y[k]=\frac{1}{k!}(\frac{d^k y(x)}{dx^k})_{x=x_0}} \tag{33}$$

$$\boldsymbol{y(x)=\sum_{k=0}^{\infty}(x-x_0)^k\, Y[k]} \tag{34}$$

Part of the transformation functions to convert the inherent equations and boundary conditions into algebraic equations are presented in Table 1.

Applying the equations in Table 1. Using the differential transformation method to Eq. (33) the resultant equations are obtained as

Table 1 Some basic theorems of DTM for equations of motion

Original function	Transformed function
$f(x)=g(x)\pm h(x)$	$F(K)=G(K)\pm H(K)$
$f(x)=\lambda g(x)$	$F(K)=\lambda G(K)$
$f(x)=g(x)h(x)$	$F(K)=\sum_{l=0}^{K}G(K-l)H(l)$
$f(x)=\frac{d^n g(x)}{dx^n}$	$F(K)=\frac{(k+n)!}{k!}G(K+n)$
$f(x)=x^n$	$F(K)=\delta(K-n)=\begin{cases}1 & k=n\\0 & k\neq n\end{cases}$

$$\begin{aligned}&\Bigg((EI)^*+\frac{2I_3\nu}{h}\tau_0-\frac{e_{31}^2}{\lambda_{33}}\\&-\mu^2\begin{pmatrix}N_p+N_T+P_{electric}\\+H+K_P+q_z+N^H\end{pmatrix}\Bigg)\frac{(k+4)!}{k!}W[k+4]\\&+\Bigg(\frac{2I_3\nu\rho_0\omega^2}{h}+\begin{pmatrix}N_p+N_T+P_{electric}\\+H+K_P+q_z+N^H\end{pmatrix}\\&+\mu^2K_w-I_1\mu^2\omega^2\Bigg)\frac{(k+2)!}{k!}W[k+2]\\&-(K_w+I_1\omega^2)W[k]=0\end{aligned} \tag{35}$$

Refining Eq. (35) the following relation can be achieved

$$W[k+4]=\frac{\begin{aligned}&-\Bigg(\frac{2I_3\nu\rho_0\omega^2}{h}+\begin{pmatrix}N_p+N_T+P_{electric}\\+H+K_P+q_z+N^H\end{pmatrix}\\&+\mu^2K_w-I_1\mu^2\omega^2\Bigg)\frac{(k+2)!}{k!}W[k+2]\\&+(K_w+I_1\omega^2)W[k]\end{aligned}}{\begin{aligned}&\Bigg((EI)^*+\frac{2I_3\nu}{h}\tau_0-\frac{e_{31}^2}{\lambda_{33}}\\&-\mu^2\begin{pmatrix}N_p+N_T+P_{electric}\\+H+K_P+q_z+N^H\end{pmatrix}\Bigg)\frac{(k+4)!}{k!}\end{aligned}} \tag{36}$$

And also the resultant equations for boundary conditions using Table 2 contents are obtained as

- Simply-Simply Supported:

$$\begin{aligned}&W[0]=0, \qquad W[2]=0\\&\sum_{k=0}^{\infty}W[k]=0, \quad \sum_{k=0}^{\infty}k(k-1)\,W[k]=0\end{aligned} \tag{37a}$$

- Clamped-Clamped:

$$\begin{aligned}&W[0]=0, \qquad W[1]=0\\&\sum_{k=0}^{\infty}W[k]=0, \quad \sum_{k=0}^{\infty}k\,W[k]=0\end{aligned} \tag{37b}$$

- Clamped-Simply:

$$\begin{aligned}&W[0]=0, \qquad W[1]=0\\&\sum_{k=0}^{\infty}W[k]=0, \quad \sum_{k=0}^{\infty}k(k-1)\,W[k]=0\end{aligned} \tag{37c}$$

- Clamped-Elastic supported (C-E):

$$\begin{aligned}&W[0]=0,\ W[1]=0,\ W[2]=C_1,\ W[3]=C_2\\&\sum_{k=0}^{\infty}EI_s k(k-1)\,W[k]\ -\sum_{k=0}^{\infty}K_{RR}k\ W[k]\ =0\\&\sum_{k=0}^{\infty}EI_s k(k-1)(k-2)\,W[k]\ +\sum_{k=0}^{\infty}K_{TR}\ W[k]\ =0\end{aligned} \tag{38a}$$

- Simply-Elastic supported (S-E):

$$\begin{aligned}&W[0]=0,\ W[2]=C_1,\ W[1]=0,\ W[3]=C_2\\&\sum_{k=0}^{\infty}EI_s k(k-1)\,W[k]\ -\sum_{k=0}^{\infty}K_{RR}k\ W[k]\ =0\end{aligned} \tag{38b}$$

Table 2 Transformed boundary conditions (B.C.) based on DTM

X = 0		X = L	
Original B.C.	Transformed B.C.	Original B.C.	Transformed B.C.
$f(0)=0$	$F[0]=0$	$f(L)=0$	$\sum_{k=0}^{\infty} F[k]=0$
$\frac{df(0)}{dx}=0$	$F[1]=0$	$\frac{\mathrm{df}(L)}{\mathrm{dx}}=0$	$\sum_{k=0}^{\infty} k\, F[k]=0$
$\frac{d^2f(0)}{\mathrm{dx}^2}=0$	$F[2]=0$	$\frac{d^2f(L)}{\mathrm{dx}^2}=0$	$\sum_{k=0}^{\infty} k(k-1)\, F[k]=0$
$\frac{d^3f(0)}{\mathrm{dx}^3}=0$	$F[3]=0$	$\frac{d^3f(L)}{\mathrm{dx}^3}=0$	$\sum_{k=0}^{\infty} k(k-1)(k-2)F[k]=0$

$$\sum_{k=0}^{\infty} EI_s k(k-1)(k-2)\; W[k] + \sum_{k=0}^{\infty} K_{TR}\; W[k] \;=0 \qquad (38b)$$

- Elastic-Elastic supported (E-E):

$$W[0]=C_1,\; W[1]=C_2,$$
$$W[2]=-\frac{K_{RL}C_2}{2EI_s},\; W[3]=\frac{K_{TL}C_1}{6EI_s}$$
$$\sum_{k=0}^{\infty} EI_s k(k-1)\; W[k] \;-\sum_{k=0}^{\infty} K_{RR}k\; W[k] \;=0 \qquad (38c)$$
$$\sum_{k=0}^{\infty}\; EI_s k(k-1)(k-2)\; W[k] + \sum_{k=0}^{\infty} K_{TR}\; W[k] \;=0$$

In this investigation, the spring constants which can be calculated in terms of Young's modulus and moment of

Table 3 Al material properties

Properties	Symbol	Al (Hosseini-Hashemi *et al*. 2013, Komijani *et al*. 2013)
Young modules	E	70 GPa
Poisn ratio	ν	0.3
Mass density	ρ	2700 Kg/m^3
Residual surface tensions	τ^0	0.9108 N.m
Elasticity surface modules	E^s	5.1882 N.m
density of surface layer	ρ^s	5.46*10^{-7} Kg.m^2
Piezoelectric coefficient	e_{31}	-10 C.m^2
Dielectric coefficient	λ_{33}	1.0275*10^{-8}

Table 4 Convergence study of the HTMP nanobeam for the first three natural frequencies ($L/h=100,\; \mu=2\mathrm{nm}^2$)

k	C-C			C-S			S-S			C-F		
	$\bar{\omega}_1$	$\bar{\omega}_2$	$\bar{\omega}_3$	$\bar{\omega}_1$	$\bar{\omega}_2$	$\bar{\omega}_3$	$\bar{\omega}_1$	$\bar{\omega}_2$	$\bar{\omega}_3$	$\bar{\omega}_1$	$\bar{\omega}_2$	$\bar{\omega}_3$
11	18.9537			14.4286			9.0384			3.5465		
13	20.4543			14.6787			9.0181			3.5470	18.4635	
15	19.9907			14.5958			9.0194	27.9180		3.5469	19.7658	
17	20.0367			14.5995			9.0194	29.9999		3.5469	19.4764	
19	20.0318			14.5991	43.1861		9.0194	29.4611		3.5469	19.5121	
21	20.0322	43.6093		14.5991	41.6494		9.0194	29.5137		3.5469	19.5088	
23	20.0321	44.5424		14.5991	41.8090		9.0194	29.5086		3.5469	19.5091	43.7193
25	20.0321	44.3698		14.5991	41.7900		9.0194	29.5090	52.7212	3.5469	19.5090	44.7237
27	20.0321	44.3893		14.5991	41.7918		9.0194	29.5090	53.3891	3.5469	19.5090	44.5335
29	20.0321	44.3873		14.5991	41.7917	75.2351	9.0194	29.5090	53.2852	3.5469	19.5090	44.5549
31	20.0321	44.3875	69.6921	14.5991	41.7917	74.7880	9.0194	29.5090	53.2962	3.5469	19.5090	44.5527
33	20.0321	44.3875	70.1564	14.5991	41.7917	74.8396	9.0194	29.5090	53.2952	3.5469	19.5090	44.5529
35	20.0321	44.3875	70.0864	14.5991	41.7917	74.8338	9.0194	29.5090	53.2952	3.5469	19.5090	44.5529
37	20.0321	44.3875	70.0943	14.5991	41.7917	74.8344	9.0194	29.5090	53.2952	3.5469	19.5090	44.5529
39	20.0321	44.3875	70.0935	14.5991	41.7917	74.8343	9.0194	29.5090	53.2952	3.5469	19.5090	44.5529
41	20.0321	44.3875	70.0936	14.5991	41.7917	74.8343	9.0194	29.5090	53.2952	3.5469	19.5090	44.5529
43	20.0321	44.3875	70.0936	14.5991	41.7917	74.8343	9.0194	29.5090	53.2952	3.5469	19.5090	44.5529

Table 5 Comparison of the non-dimensional fundamental frequency for a nanobeam with various nonlocal parameters with S-S boundary conditions ($L/h = 100,\ K_{RR} \to 0,\ K_{TR} \to \infty$)

μ	S-S Boundary condition		
	Present paper	Reddy (2007)	Eltaher *et al*. (2013)
0	9.8696	9.8696	9.8700
1	9.4158	9.4159	9.4162
2	9.0194	9.0195	9.0197
3	8.6691	8.6693	8.6695
4	8.3569	8.3569	8.3571
5	8.0760	8.0761	8.0762

inertia (I) from the following equations, $K_{TL} = \frac{\beta_{TL} EI_s}{L^3}$, $K_{RL} = \frac{\beta_{RL} EI_s}{L}$, $K_{TR} = \frac{\beta_{TR} EI_s}{L^3}$ and $K_{RR} = \frac{\beta_{RR} EI_s}{L}$, in which the corresponding values of β are the given parameters of spring constant factors.

5. Results and discussion

This section is devoted to results obtained from analysis of hygro-thermo-electromagnetic mechanical vibration behavior of nanobeam taking into account surface effect and the nonlocal parameter for various non-ideal elastic boundary conditions based on the Euler–Bernoulli beam theory. Supposing the nanobeam is made of AL and the material properties are given in Table 3. In order to make sure that the convergence of obtained frequencies, a number of iterations k for first three natural frequencies is chosen and the results are studied in Table 4.

To validate the DTM results and solution mechanism, the peer-reviewed references are presented in this section. The first one is related to the dimensionless natural frequency for simply-simply boundary condition is expressed in (Reddy 2007) and (Eltaher *et al*. 2013) are organized in Table 5. As it is indicated from Table 5 the results are more compatible with (Reddy 2007) than (Eltaher *et al*. 2013), the difference in the results of these sources is because of solution method. The results in (Reddy 2007) are acquired by analytical solution approach

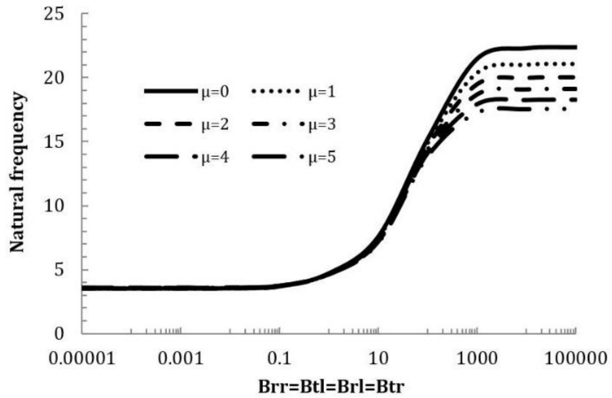

Fig. 2 Natural frequency for different spring constant factors for C-E and nonlocal parameters without considering surface effect

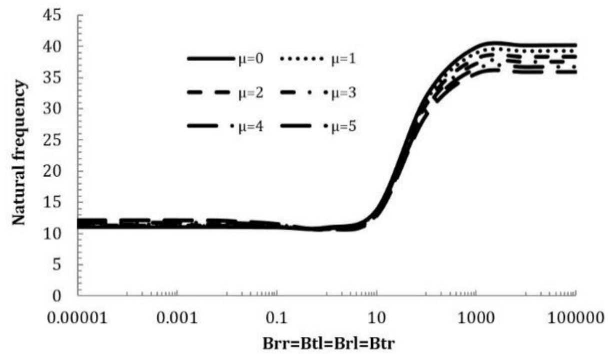

Fig. 3 Natural frequency for different spring constant factors for C-E and nonlocal parameters by considering surface effect

which are more definitive in comparison with those presented in (Eltaher *et al*. 2013) which are acquired by finite element method (FEM). Table 6 indicates the same results presented for clamp-simply, clamp-clamp and clamp-free boundary conditions and compared only with Eltaher's finite element study.

After investigating the convergence and validation of the results, the influence of spring constant factors β with changing nonlocal parameters both in presence and absence of the surface effect for C-E, S-E and E-E boundary conditions is illustrated in Figs. 2-7. As it is indicated in

Table 6 Comparison of the non-dimensional fundamental frequency for a nanobeam with various nonlocal parameters with C-S boundary conditions (with C-C boundary conditions ($L/h = 100, K_{RR} = K_{TR} \to \infty$), with C-S boundary conditions ($L/h = 100,\ K_{RR} \to 0,\ K_{TR} \to \infty$) and with C-F boundary conditions ($L/h = 100,\ K_{RR} = K_{TR} \to 0$)

μ	C-S		C-C		C-F	
	Present paper	Eltaher *et al*. (2013)	Present paper	Eltaher *et al*. (2013)	Present paper	Eltaher *et al*. (2013)
0	15.4182	15.4189	22.3734	22.3744	3.5160	3.5161
1	14.9924	14.9929	21.1091	21.1096	3.5312	3.5314
2	14.5992	14.5997	20.0329	20.0330	3.5469	3.5470
3	14.2349	14.2353	19.103	19.1028	3.5629	3.5630
4	13.8962	13.8965	18.2895	18.2890	3.5794	3.5795
5	13.5801	13.5803	17.5702	17.5696	3.5794	3.5963

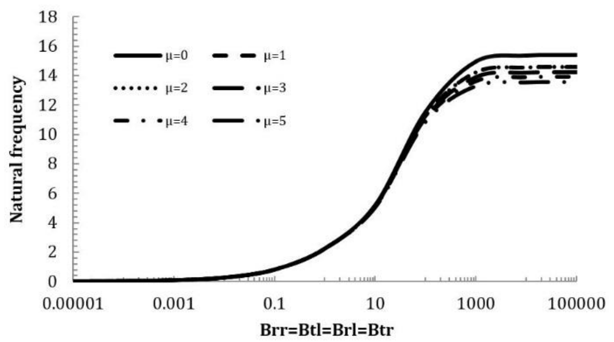

Fig. 4 Natural frequency for different spring constant factors for S-E and nonlocal parameters without considering surface effect

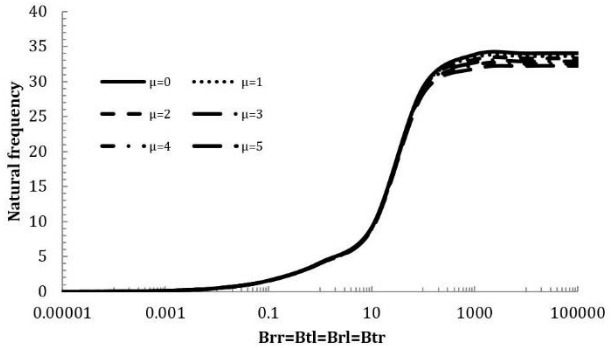

Fig. 5 Natural frequency for different spring constant factors for S-E and nonlocal parameters by considering surface effect

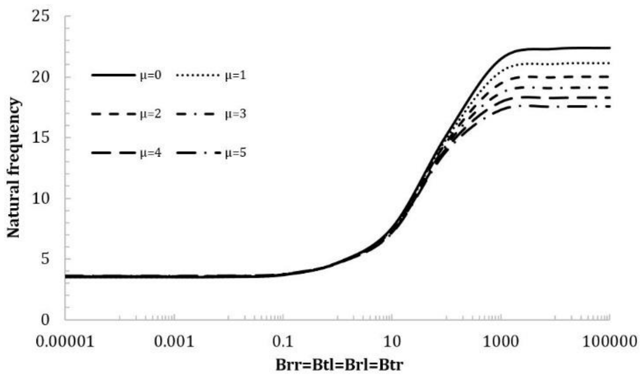

Fig. 6 Natural frequency for different spring constant factors for E-E and nonlocal parameters without considering surface effect

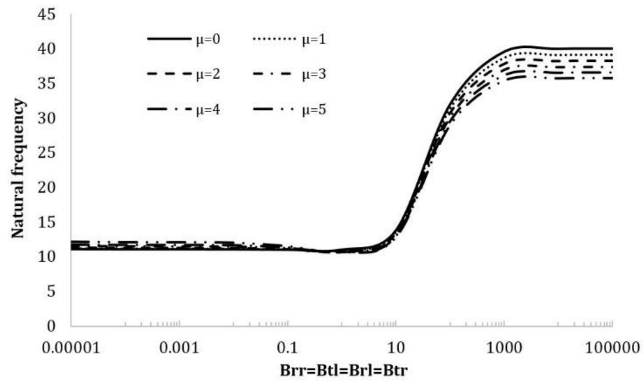

Fig. 7 Natural frequency for different spring constant factors for E-E and nonlocal parameters by considering surface effect

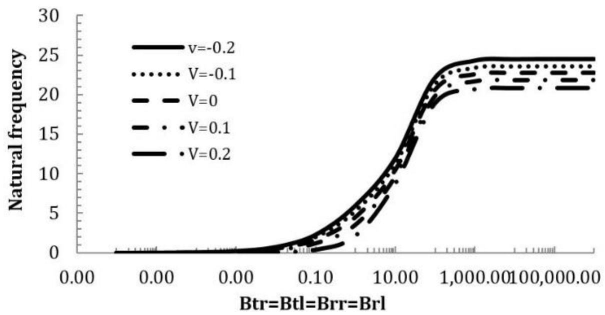

Fig. 8 Natural frequency for different spring constant factors for C-E and external voltage by considering surface effect

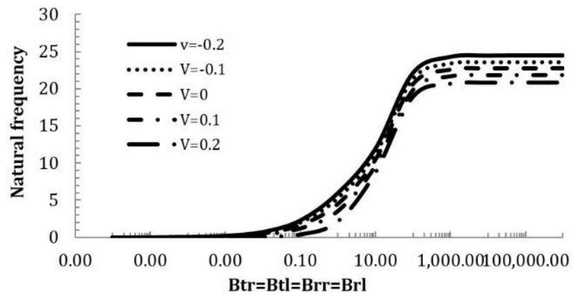

Fig. 9 Natural frequency for different spring constant factors for S-E and external voltage by considering surface effect

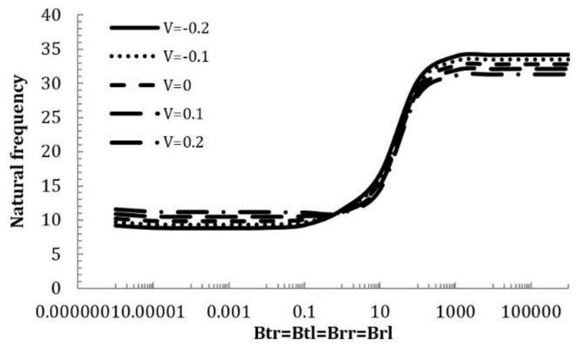

Fig. 10 Natural frequency for different spring constant factors for E-E and external voltage by considering surface effect

Figs. 2-7, increasing spring constant factor leads to increase in natural frequency. The increase in frequencies are slightly in lower factors and after it reaches to 1, goes up suddenly and at the very larger amount of β, the natural frequencies change slightly again. The increasing reason is that higher amount of spring constant factors cause more stiffness in nanobeam and higher frequencies, respectively. It is noteworthy that while increasing the nonlocal parameter, it can be shown considerable decreasing in natural frequencies due to reducing of the nanobeam stiffness in the presence of nonlocal effects.

Table 7 First natural frequency of piezoelectric nanobeam for temperature change with various boundary condition ($L = 20\ nm,\ L/h = 10,\ h/b = 2,\ V = 0.5,\ \mu = 2nm^2$)

β	ΔT						
	0	10	50	100	150	200	300
				S-E			
10^{-6}	0.0008	0.0009	0.0010	0.0012	0.0013	0.0014	0.0016
10^{-5}	0.0026	0.0027	0.0032	0.0037	0.0041	0.0044	0.0051
10^{-4}	0.0083	0.0087	0.0101	0.0116	0.0129	0.0141	0.0162
10^{-3}	0.0264	0.0276	0.0319	0.0366	0.0408	0.0445	0.0512
10^{-2}	0.0870	0.0906	0.1038	0.1182	0.1310	0.1426	0.1635
10^{-1}	0.3623	0.3704	0.4013	0.4368	0.4696	0.5003	0.5565
1	2.0900	2.0984	2.1321	2.1734	2.2139	2.2537	2.3311
10^{1}	8.6518	8.6561	8.6734	8.6950	8.7165	8.7380	8.7808
10^{2}	18.8807	18.8846	18.9004	18.9202	18.9399	18.9596	18.9989
10^{3}	20.6738	20.6782	20.6957	20.7176	20.7394	20.7612	20.8047
10^{4}	20.8232	20.8277	20.8453	20.8673	20.8893	20.9113	20.9551
10^{5}	20.8379	20.8423	20.8599	20.8819	20.9039	20.9259	20.9698
10^{6}	20.8393	20.8437	20.8614	20.8834	20.9054	20.9274	20.9713
				C-E			
10^{-6}	11.2168	11.2132	11.1989	11.1811	11.1634	11.1458	11.1107
10^{-5}	11.2168	11.2132	11.1989	11.1811	11.1634	11.1458	11.1107
10^{-4}	11.2167	11.2132	11.1989	11.1811	11.1633	11.1457	11.1107
10^{-3}	11.2161	11.2125	11.1982	11.1805	11.1628	11.1452	11.1102
10^{-2}	11.2097	11.2062	11.1922	11.1747	11.1574	11.1401	11.1057
10^{-1}	11.1550	11.1521	11.1404	11.1259	11.1114	11.0970	11.0685
1	11.0787	11.0789	11.0795	11.0804	11.0813	11.0822	11.0841
10^{1}	14.4191	14.4218	14.4326	14.4461	14.4595	14.473	14.4998
10^{2}	28.1328	28.1354	28.1456	28.1584	28.1712	28.1839	28.2095
10^{3}	31.1273	31.1305	31.1435	31.1597	31.1759	31.1921	31.2244
10^{4}	31.3003	31.3036	31.3167	31.3331	31.3495	31.3658	31.3986
10^{5}	31.3167	31.3199	31.3331	31.3495	31.3659	31.3823	31.4150
10^{6}	31.3183	31.3216	31.3347	31.3511	31.3675	31.3839	31.4167
				E-E			
10^{-6}	11.6153	11.6117	11.5974	11.5796	11.5618	11.5442	11.5091
10^{-5}	11.2554	11.2518	11.2375	11.2197	11.202	11.1843	11.1492
10^{-4}	11.2206	11.217	11.2027	11.1849	11.1672	11.1495	11.1145
10^{-3}	11.2165	11.2129	11.1986	11.1809	11.1632	11.1456	11.1106
10^{-2}	11.2098	11.2062	11.1922	11.1748	11.1574	11.1401	11.1058
10^{-1}	11.1550	11.1521	11.1404	11.1259	11.1114	11.0970	11.0685
1	11.0787	11.0789	11.0795	11.0804	11.0813	11.0822	11.0841
10^{1}	14.4191	14.4218	14.4326	14.4461	14.4595	14.4730	14.4998
10^{2}	28.1328	28.1354	28.1456	28.1584	28.1712	28.1839	28.2095
10^{3}	31.1273	31.1305	31.1435	31.1597	31.1759	31.1921	31.2244
10^{4}	31.3003	31.3036	31.3167	31.3331	31.3495	31.3658	31.3986
10^{5}	31.3167	31.3199	31.3331	31.3495	31.3659	31.3823	31.415
10^{6}	31.3183	31.3216	31.3347	31.3511	31.3675	31.3839	31.4167

Table 8 First natural frequency for piezoelectric nanobeam by considering magnetic field with various boundary condition ($L = 20\ nm,\ L/h = 10,\ h/b = 2,\ V = 0.5,\ \mu = 2nm^2$)

β	ΔT						
	0	10	50	100	150	200	300
S-E							
10^{-6}	0.0054	0.0054	0.0054	0.0054	0.0055	0.0055	0.0055
10^{-5}	0.0170	0.0170	0.0171	0.0171	0.0172	0.0174	0.0175
10^{-4}	0.0537	0.0538	0.0540	0.0542	0.0545	0.0549	0.0553
10^{-3}	0.1699	0.1702	0.1707	0.1714	0.1724	0.1735	0.1748
10^{-2}	0.5359	0.5368	0.5385	0.5408	0.5437	0.5473	0.5515
10^{-1}	1.6567	1.6597	1.6647	1.6716	1.6805	1.6913	1.7040
1	4.4943	4.5011	4.5124	4.5281	4.5483	4.5728	4.6016
10^{1}	10.4140	10.4203	10.4307	10.4453	10.4640	10.4868	10.5137
10^{2}	20.5723	20.5786	20.5890	20.6037	20.6224	20.6453	20.6724
10^{3}	22.5639	22.5710	22.5828	22.5993	22.6205	22.6463	22.6769
10^{4}	22.7282	22.7354	22.7473	22.7639	22.7853	22.8114	22.8422
10^{5}	22.7443	22.7514	22.7633	22.7800	22.8014	22.8275	22.8583
10^{6}	22.7459	22.7530	22.7649	22.7816	22.8030	22.8291	22.8599
C-E							
10^{-6}	9.8564	9.8519	9.8444	9.8339	9.8204	9.8040	9.7848
10^{-5}	9.8564	9.8519	9.8444	9.8339	9.8205	9.8041	9.7848
10^{-4}	9.8566	9.8521	9.8446	9.8341	9.8207	9.8043	9.7850
10^{-3}	9.8586	9.8541	9.8466	9.8362	9.8227	9.8064	9.7871
10^{-2}	9.8784	9.8740	9.8667	9.8564	9.8433	9.8273	9.8085
10^{-1}	10.0637	10.0601	10.0543	10.0461	10.0356	10.0228	10.0077
1	11.2440	11.2449	11.2465	11.2487	11.2516	11.2551	11.2593
10^{1}	15.5925	15.5969	15.6042	15.6146	15.6278	15.6440	15.6631
10^{2}	29.2546	29.2589	29.2660	29.2759	29.2887	29.3042	29.3226
10^{3}	32.5585	32.5640	32.5731	32.5858	32.6022	32.6223	32.6459
10^{4}	32.7491	32.7546	32.7639	32.7768	32.7934	32.8137	32.8377
10^{5}	32.7671	32.7726	32.7819	32.7948	32.8114	32.8317	32.8557
10^{6}	32.7689	32.7744	32.7836	32.7966	32.8132	32.8335	32.8575
E-E							
10^{-6}	10.2501	10.2455	10.2380	10.2274	10.2139	10.1974	10.1780
10^{-5}	9.8941	9.8896	9.8821	9.8716	9.8581	9.8417	9.8224
10^{-4}	9.8604	9.8559	9.8484	9.8379	9.8244	9.8080	9.7887
10^{-3}	9.8590	9.8545	9.8470	9.8365	9.8231	9.8068	9.7875
10^{-2}	9.8784	9.8740	9.8667	9.8565	9.8433	9.8273	9.8085
10^{-1}	10.0637	10.0602	10.0543	10.0461	10.0356	10.0228	10.0077
1	11.2440	11.2449	11.2465	11.2487	11.2516	11.2551	11.2593
10^{1}	15.5925	15.5969	15.6042	15.6146	15.6278	15.6440	15.6631
10^{2}	29.2546	29.2589	29.2660	29.2759	29.2887	29.3042	29.3226
10^{3}	32.5585	32.5640	32.5731	32.5858	32.6022	32.6223	32.6459
10^{4}	32.7491	32.7546	32.7639	32.7768	32.7934	32.8137	32.8377
10^{5}	32.7671	32.7726	32.7819	32.7948	32.8114	32.8317	32.8557
10^{6}	32.7689	32.7744	32.7836	32.7966	32.8132	32.8335	32.8575

Table 9 First natural frequency of piezoelectric nanobeam for various axial load with various boundary condition ($L = 20\ nm,\ L/h = 10,\ \ h/b = 2,\ V = 0.5,\ \mu = 2nm^2,\ T = 20$)

β	$N_p = -1$	$N_p = -0.5$	$N_p = 0$	$N_p = 0.5$	$N_p = 1$
			S-E		
10^{-6}	0.0009	0.0013	0.0016	0.0018	0.0020
10^{-5}	0.0030	0.0041	0.0050	0.0058	0.0064
10^{-4}	0.0094	0.0131	0.0159	0.0182	0.0203
10^{-3}	0.0298	0.0414	0.0502	0.0577	0.0642
10^{-2}	0.0946	0.1309	0.1588	0.1822	0.2028
10^{-1}	0.3087	0.4161	0.5001	0.5712	0.6338
1	1.1491	1.3578	1.5373	1.6969	1.8418
10^{1}	4.2452	4.3904	4.5303	4.6654	4.7962
10^{2}	10.6990	10.8250	10.9479	11.0678	11.1849
10^{3}	13.6383	13.8321	14.0227	14.2102	14.3947
10^{4}	13.9777	14.1817	14.3825	14.5804	14.7753
10^{5}	14.0117	14.2167	14.4185	14.6174	14.8135
10^{6}	14.0151	14.2202	14.4221	14.6211	14.8173
			C-E		
10^{-6}	3.9997	3.9265	3.8554	3.7862	3.7190
10^{-5}	3.9997	3.9265	3.8554	3.7863	3.7190
10^{-4}	3.9997	3.9266	3.8555	3.7864	3.7191
10^{-3}	4.0004	3.9273	3.8564	3.7874	3.7203
10^{-2}	4.0067	3.9350	3.8654	3.7977	3.7320
10^{-1}	4.0684	4.0089	3.9516	3.8965	3.8434
1	4.5554	4.5703	4.5868	4.6049	4.6243
10^{1}	6.9178	7.0089	7.0988	7.1875	7.2753
10^{2}	14.7134	14.7787	14.8434	14.9075	14.9710
10^{3}	20.5514	20.6797	20.8069	20.9329	21.0579
10^{4}	21.2879	21.4304	21.5717	21.7121	21.8514
10^{5}	21.3605	21.5044	21.6472	21.7890	21.9298
10^{6}	21.3677	21.5117	21.6547	21.7967	21.9376
			E-E		
10^{-6}	4.8077	4.7451	4.6840	4.6242	4.5657
10^{-5}	4.0642	3.9913	3.9205	3.8515	3.7844
10^{-4}	4.0060	3.9329	3.8619	3.7927	3.7255
10^{-3}	4.0010	3.9280	3.8570	3.7880	3.7209
10^{-2}	4.0068	3.9351	3.8654	3.7978	3.7320
10^{-1}	4.0684	4.0089	3.9516	3.8965	3.8435
1	4.5554	4.5703	4.5868	4.6049	4.6243
10^{1}	6.9178	7.0089	7.0988	7.1875	7.2753
10^{2}	14.7134	14.7787	14.8434	14.9075	14.9710
10^{3}	20.5514	20.6797	20.8069	20.9329	21.0579
10^{4}	21.2879	21.4304	21.5717	21.7121	21.8514
10^{5}	21.3605	21.5044	21.6472	21.7890	21.9298
10^{6}	21.3677	21.5117	21.6547	21.7967	21.9376

Table 10 First natural frequency of piezoelectric nanobeam for various temperature change and moisture effect with various boundary condition ($L = 20\,nm,\ L/h = 10,\ h/b = 2,\ V = 0.5,\ \mu = 2\,nm^2$)

β	T = 0			T = 10			T = 50		
	%ΔH = 0	%ΔH = 10	%ΔH = 20	%ΔH = 0	%ΔH = 10	%ΔH = 20	%ΔH = 0	%ΔH= 1 0	%ΔH= 2 0
					S-E				
10^{-6}	0.0053	0.0053	0.0053	0.0053	0.0053	0.0053	0.0054	0.0054	0.0054
10^{-5}	0.0169	0.0169	0.0168	0.0169	0.0169	0.0169	0.0170	0.0170	0.0169
10^{-4}	0.0534	0.0533	0.0533	0.0535	0.0534	0.0533	0.0537	0.0536	0.0535
10^{-3}	0.1689	0.1686	0.1684	0.1690	0.1688	0.1686	0.1698	0.1695	0.1693
10^{-2}	0.5327	0.5320	0.5312	0.5333	0.5325	0.5318	0.5355	0.5348	0.5340
10^{-1}	1.6472	1.6449	1.6426	1.6489	1.6466	1.6443	1.6557	1.6534	1.6511
1	4.4728	4.4676	4.4624	4.4766	4.4714	4.4663	4.4920	4.4869	4.4817
10^{1}	10.3942	10.3895	10.3847	10.3978	10.3930	10.3883	10.4120	10.4072	10.4025
10^{2}	20.5525	20.5477	20.5430	20.5560	20.5513	20.5465	20.5702	20.5655	20.5607
10^{3}	22.5415	22.5362	22.5308	22.5455	22.5402	22.5348	22.5615	22.5562	22.5508
10^{4}	22.7057	22.7003	22.6948	22.7097	22.7043	22.6989	22.7259	22.7205	22.7150
10^{5}	22.7217	22.7163	22.7109	22.7257	22.7203	22.7149	22.7419	22.7365	22.7311
10^{6}	22.7233	22.7179	22.7124	22.7273	22.7219	22.7165	22.7435	22.7381	22.7327
					C-E				
10^{-6}	9.8707	9.8742	9.8776	9.8682	9.8716	9.8750	9.8579	9.8613	9.8648
10^{-5}	9.8707	9.8742	9.8776	9.8682	9.8716	9.8750	9.8579	9.8614	9.8648
10^{-4}	9.8709	9.8744	9.8778	9.8684	9.8718	9.8752	9.8581	9.8616	9.8650
10^{-3}	9.8729	9.8763	9.8797	9.8703	9.8738	9.8772	9.8601	9.8635	9.8670
10^{-2}	9.8924	9.8957	9.8991	9.8899	9.8932	9.8966	9.8799	9.8832	9.8866
10^{-1}	10.0749	10.0776	10.0803	10.0729	10.0756	10.0782	10.0649	10.0675	10.0702
1	11.2410	11.2403	11.2396	11.2415	11.2408	11.2401	11.2436	11.2429	11.2422
10^{1}	15.5785	15.5751	15.5718	15.5810	15.5776	15.5743	15.5910	15.5876	15.5843
10^{2}	29.2412	29.2379	29.2347	29.2436	29.2403	29.2371	29.2532	29.2500	29.2467
10^{3}	32.5412	32.5370	32.5329	32.5443	32.5401	32.5360	32.5567	32.5525	32.5484
10^{4}	32.7316	32.7274	32.7232	32.7347	32.7305	32.7263	32.7472	32.7431	32.7389
10^{5}	32.7495	32.7453	32.7411	32.7527	32.7485	32.7443	32.7652	32.7610	32.7568
10^{6}	32.7513	32.7471	32.7429	32.7544	32.7502	32.7460	32.7670	32.7628	32.7586
					E-E				
10^{-6}	9.8707	9.8742	9.8776	9.8682	9.8716	9.8750	9.8579	9.8613	9.8648
10^{-5}	9.8707	9.8742	9.8776	9.8682	9.8716	9.8750	9.8579	9.8614	9.8648
10^{-4}	9.8709	9.8744	9.8778	9.8684	9.8718	9.8752	9.8581	9.8616	9.8650
10^{-3}	9.8729	9.8763	9.8797	9.8703	9.8738	9.8772	9.8601	9.8635	9.8670
10^{-2}	9.8924	9.8957	9.8991	9.8899	9.8932	9.8966	9.8799	9.8832	9.8866
10^{-1}	10.0749	10.0776	10.0803	10.0729	10.0756	10.0782	10.0649	10.0675	10.0702
1	11.2410	11.2403	11.2396	11.2415	11.2408	11.2401	11.2436	11.2429	11.2422
10^{1}	15.5785	15.5751	15.5718	15.5810	15.5776	15.5743	15.5910	15.5876	15.5843
10^{2}	29.2412	29.2379	29.2347	29.2436	29.2403	29.2371	29.2532	29.2500	29.2467
10^{3}	32.5412	32.5370	32.5329	32.5443	32.5401	32.5360	32.5567	32.5525	32.5484
10^{4}	32.7316	32.7274	32.7232	32.7347	32.7305	32.7263	32.7472	32.7431	32.7389
10^{5}	32.7495	32.7453	32.7411	32.7527	32.7485	32.7443	32.7652	32.7610	32.7568
10^{6}	32.7513	32.7471	32.7429	32.7544	32.7502	32.7460	32.7670	32.7628	32.7586

The variation of the temperature and its effect on the first natural frequency in the constant nonlocal parameter ($\mu = 2$) and various boundary conditions is reported in Table 7. Enlargement in the temperature leads to higher first natural frequency by an increase in the nanobeam stiffness. According to the Figs. 8-10. increasing in applied voltage from negative to positive decline the amount of first natural frequency. Furthermore, the negative voltage tends to enhance natural frequency while the positive voltage makes lower natural frequencies. This phenomenon is because of the fact that positive and negative voltage generate compressive and tensile forces in nanobeams, respectively. The effect of external magnetic potential on the first natura vibration frequency is explored in Table 8 For three distinct boundary conditions. As a consequence, it can be observed in Table 8, there is a tiny increase in natural frequency while the magnetic potential is increasing and it means that the higher values of leads to higher beam stiffness like enlargement in vibration temperature.

Influence of axial preload has been illustrated in Table 9. It should be noted that when the axial compressive force is applied, natural frequency tends to lower values and for axial tensile force, natural frequency increases. This event is because of the nanobeam strengthening and weakening of the axial tensile and compressive forces, respectively. Table 10. Presents the effects of hygro-thermal loads on the first natural frequency. It is observable that the increase of moisture and temperature results in reduction in plate stiffness and consequently in the natural frequency and the variation of natural frequency is more dependable on the boundary condition since in the C-C condition, the changing in natural frequency is almost minor and can be neglected but in other boundary conditions, disparity is more important and considerable. Thus, moisture concentration in the presence of thermal load has a softening impact on the nanobeam and would be considered in the analysis.

6. Conclusions

In this paper, Eringen nonlocal beam theory was put to use to investigate the hygro–thermo–electromagnetic mechanical vibration characteristic of nanobeam rested on the elastic foundation for non-ideal boundary conditions by considering surface effects. The rotational and transitional springs at each end which apply small deflections and moments were implemented to assume the elastic boundary condition. the governing equation was derived by Hamilton's principle and the natural frequencies were determined by DTM which is a suitable tool to solve differential equations. Based on the above mentioned numerical results, the conclusions are as follows:

- Increasing the spring constants from 10^{-6} to 10^{6} causes an increase in the natural frequencies for all boundary conditions.
- The natural frequencies decrease while the nonlocal parameter increases.
- Rising the temperature leads to increase in the natural frequencies. The intensity of change in natural frequency is more considerable at lower spring constants.
- Increasing the applied voltage from negative to positive decline the amount of first natural frequency.
- DTM method gives faster convergence compare with other classical approaches.
- As axial compressive force is applied, natural frequency tends to lower values and for axial tensile force, natural frequency tends to increase.
- Both of moisture concentration and magnetic potential result in reduction in plate stiffness and consequently in the natural frequency but the moisture effect on the behavior of the nanobeam is more dependable on the boundary condition and its specifications.

References

Aydogdu, M. (2009), "A general nonlocal beam theory: its application to nanobeam bending, buckling and vibration", *Physica E*: *Low-dimens*. *Syst*. *Nanostruct*., **41**(9), 1651-1655. https://doi.org/10.1016/j.physe.2009.05.014

Bailey, T. and Ubbard, J.E. (1985), "Distributed piezoelectric-polymer active vibration control of a cantilever beam", *J*. *Guidance*, *Control*, *and Dynamics*, **8**(5), 605-611. https://doi.org/10.2514/3.20029

Barari, A., Kaliji, H.D., Ghadimi, M. and Domairry, G. (2011), "Non-linear vibration of Euler-Bernoulli beams", *Latin Am*. *J*. *Solids Struct*., **8**(2), 139-148. https://doi.org/10.1590/S1679-78252011000200002

Bauchau, O.A. and Craig, J.I. (2009), "Euler-Bernoulli beam theory", In: *Structural Analysis*, Springer, pp. 173-221.

Ebrahimi, F. and Barati, M.R. (2017), "Small-scale effects on hygro-thermo-mechanical vibration of temperature-dependent nonhomogeneous nanoscale beams", *Mech*. *Adv*. *Mater*. *Struct*., **24**(11), 924-936. https://doi.org/10.1080/15376494.2016.1196795

Ebrahimi, F., Shaghaghi, G.R. and Salari, E. (2014), "Vibration analysis of size-dependent nano beams based on nonlocal Timoshenko Beam Theory", *J*. *Mech*. *Eng*. *Technol*. (*JMET*), **6**(2).

Eltaher, M.A., Alshorbagy, A.E. and Mahmoud, F.F. (2013), "Vibration analysis of Euler--Bernoulli nanobeams by using finite element method", *Appl*. *Mathe*. *Model*., **37**(7), 4787-4797. https://doi.org/10.1016/j.apm.2012.10.016

Eringen, A.C. (1983), "On differential equations of nonlocal elasticity and solutions of screw dislocation and surface waves", *J*. *Appl*. *Phys*., **54**(9), 4703-4710. https://doi.org/10.1063/1.332803

Friesen, C., Dimitrov, N., Cammarata, R.C. and Sieradzki, K. (2001), "Surface stress and electrocapillarity of solid electrodes", *Langmuir*, **17**(3), 807-815. https://doi.org/10.1021/la000911m

Gayen, D. and Roy, T. (2013), "Hygro-thermal effects on stress analysis of tapered laminated composite beam", *Int*. *J*. *Compos*. *Mater*., **3**(3), 46-55. https://doi.org/10.5923/j.cmaterials.20130303.02

Gurtin, M.E. and Murdoch, A.I. (1975), "A continuum theory of elastic material surfaces", *Arch*. *Rational Mech*. *Anal*., **57**(4), 291-323. https://doi.org/10.1007/BF00261375

He, J. and Lilley, C.M. (2008), "Surface effect on the elastic behavior of static bending nanowires", *Nano Lett*., **8**(7), 1798-1802. https://doi.org/10.1021/nl0733233

Henderson, J.P., Plummer, A. and Johnston, N. (2018), "An electro-hydrostatic actuator for hybrid active-passive vibration isolation", *Int. J. Hydromechatron.*, **1**(1), 47-71.

Hosseini-Hashemi, S., Fakher, M. and Nazemnezhad, R. (2013), "Surface effects on free vibration analysis of nanobeams using nonlocal elasticity: A comparison between Euler-Bernoulli and Timoshenko", *J. Solid Mech.*, **5**(3), 290-304.

Huang, G.-Y. and Yu, S.-W. (2006), "Effect of surface piezoelectricity on the electromechanical behaviour of a piezoelectric ring", *Physica Status Solidi* (*b*), **243**(4). https://doi.org/10.1002/pssb.200541521

Ke, L.L., Xiang, Y., Yang, J. and Kitipornchai, S. (2009), "Nonlinear free vibration of embedded double-walled carbon nanotubes based on nonlocal Timoshenko beam theory", *Computati. Mater. Sci.*, **47**(2), 409-417. https://doi.org/10.1016/j.commatsci.2009.09.002

Komijani, M., Kiani, Y., Esfahani, S.E. and Eslami, M.R (2013), "Vibration of thermo-electrically post-buckled rectangular functionally graded piezoelectric beams", *Compos. Struct.*, **98**, 143-152. https://doi.org/10.1016/j.compstruct.2012.10.047

Lee, U. and Kim, J. (2000), "Determination of nonideal beam boundary conditions: a spectral element approach", *AIAA Journal*, **38**(2), p. 309. https://doi.org/10.2514/2.958

Levinson, M. (1981), "A new rectangular beam theory", *J. Sound Vib.*, **74**(1), 81-87. https://doi.org/10.1016/0022-460X(81)90493-4

Li, X.Y., Wang, Z.K. and Huang, S.H. (2004), "Love waves in functionally graded piezoelectric materials", *Int. J. Solids Struct.*, **41**(26), 7309-7328. https://doi.org/10.1016/j.ijsolstr.2004.05.064

Marzbanrad, J., Boreiry, M. and Shaghaghi, G.R. (2016), "Thermo-electro-mechanical vibration analysis of size-dependent nanobeam resting on elastic medium under axial preload in presence of surface effect", *Appl. Phys. A*, **122**(7), p. 691. https://doi.org/10.1007/s00339-016-0218-1

Marzbanrad, J., Boreiry, M. and Shaghaghi, G.R. (2017), "Surface effects on vibration analysis of elastically restrained piezoelectric nanobeams subjected to magneto-thermo-electrical field embedded in elastic medium", *Appl. Phys. A*, **123**(4), p. 246. https://doi.org/10.1007/s00339-017-0768-x

Pakdemirli, M. and Boyaci, H. (2001), "Vibrations of a stretched beam with non-ideal boundary conditions", *Mathe. Computat. Applicat.*, **6**(3), 217-220. https://doi.org/10.3390/mca6030217

Pakdemirli, M. and Boyaci, H. (2003), "Non-linear vibrations of a simple--simple beam with a non-ideal support in between", *J. Sound Vib.*, **268**(2), 331-341. https://doi.org/10.1016/S0022-460X(03)00363-8

Park, S.K. and Gao, X.L. (2006), "Bernoulli--Euler beam model based on a modified couple stress theory", *J. Micromech. Microeng.*, **16**(11), p. 2355. https://doi.org/10.1088/0960-1317/16/11/015

Rao, S.S. (2007), *Vibration of Continuous Systems*, John Wiley & Sons.

Reddy, J.N. (2007), "Nonlocal theories for bending, buckling and vibration of beams", *Int. J. Eng. Sci.*, **45**(2), 288-307. https://doi.org/10.1016/j.ijengsci.2007.04.004

Samaei, A.T., Bakhtiari, M. and Wang, G.-F. (2012), "Timoshenko beam model for buckling of piezoelectric nanowires with surface effects", *Nanoscale Res. Lett.*, **7**(1), p. 201. https://doi.org/10.1186/1556-276X-7-201

Schmid, M., Hofer, W., Varga, P., Stoltze, P., Jacobsen, K.W. and No, J.K. (1995), "Surface stress, surface elasticity, and the size effect in surface segregation", *Phys. Rev. B*, **51**(16), p. 10937. https://doi.org/10.1103/PhysRevB.51.10937

Tanaka, Y. (2018), "Active vibration compensator on moving vessel by hydraulic parallel mechanism", *Int. J. Hydromechatron.*, **1**(3), 350-359.

Tounsi, A., Benguediab, S., Adda, B., Semmah, A. and Zidour, M. (2013), "Nonlocal effects on thermal buckling properties of double-walled carbon nanotubes", *Adv. Nano Res., Int. J.*, **1**(1), 1-11. https://doi.org/10.12989/anr.2013.1.1.001

Wang, C.M., Tan, V.B.C. and Zhang, Y.Y. (2006), "Timoshenko beam model for vibration analysis of multi-walled carbon nanotubes", *J. Sound Vib.*, **294**(4), 1060-1072. https://doi.org/10.1021/nl035198a

Wang, Z., Xie, Z. and Huang, W. (2018), "A pin-moment model of flexoelectric actuators", *Int. J. Hydromechatron.*, **1**(1), 72-90.

Zhao, M.-H., Wang, Z.-L. and Mao, S.X. (2004), "Piezoelectric characterization of individual zinc oxide nanobelt probed by piezoresponse force microscope", *Nano Lett.*, **4**(4), 587-590. https://doi.org/10.1021/nl035198a

CC